Cell Signaling Analysis of Metastatic Triple Negative Breast Cancer Following Dual PI3K/mTOR Inhibitor (PIKTOR)

A Thesis submitted in partial fulfillment of the requirements for the degree of Master of Science at George Mason University

by

Tuong Vi V. Nguyen
Bachelor of Science
George Mason University, 2020

Director: Virginia Espinia, Professor
Department of Biology

Spring Semester 2021
George Mason University
Fairfax, VA

ACKNOWLEDGEMENTS

I would like to say thank you to all the participating patients and families from the Baylor Medical center. Thank you, Dr. Joyce O'Shaughnessy and Lavin Maren from the Baylor Scott and White research institute, for their work in setting up and leading the PIKTOR phase II clinical trial. Dr.Lang, Dr.Hendricks, Dr. Zismann, from The Translational Genomics Research Institute (TGEN) provided valuable NGS data. Everyone from the CAPMM lab who have helped me throughout my 2 years doing research at Mason.

A special thank you to Dr. Espina and Dr. Mueller for teaching me the scientific methods and how to best apply it throughout my project. I appreciate all your hours spent teaching me the best experimental practices, data analyzing techniques, and overall life advise.

TABLE OF CONTENTS

LIST OF TABLES

LIST OF FIGURES

LIST OF ABBREVIATIONS

Basal-like ..... BL
Breast Cancer ..... BC
Cisplatin ..... Cis
Copy Number Alterations ..... CNAs
DNA Damage Repair Deficiency ..... DDRD
Estrogen Receptor ..... ER
Homologous Recombination ..... HR
Laser Capture Microdissection ..... LCM
Luminal Androgen Receptor ..... LAR
Metastatic ..... Met
Mitogen Activated Protein Kinase ..... MAPK
Nab Paclitaxel ..... Nab-pac
Next Generation Sequencing ..... NGS
Nonhomologous End Joining ..... NHEJ
Progesterone Receptor ..... PR
Progression Free Survival ..... PFS
Progression of Disease ..... PD
Reverse Phase Protein Array ..... RPPA
Stable Disease ..... SD
Triple Negative Breast Cancer ..... TNBC
Tumor Mutational Burden ..... TMB

ABSTRACT

CELL SIGNALING ANALYSIS OF METASTATIC TRIPLE NEGATIVE BREAST CANCER FOLLOWING DUAL PI3K/MTOR INHIBITOR (PIKTOR)

Tuong Vi V. Nguyen, M.S

George Mason University, 2021

Thesis Director: Dr. Virginia Espinia

Triple negative breast cancer (TNBC) is defined by deficient estrogen, progesterone and HER2 receptor expression, excluding TNBC patients from effective targeted therapies for breast cancer. Advancement in targeted therapy for pro-survival pathways like PI3K/AKT/mTOR (PAM) and mitogen activated protein kinase (MAPK), has shown to improve outcomes for select TNBC patients. However, targeted therapies have not produced complete responses in the majority of patients and there is high degree of systemic relapse following conventional neoadjuvant chemotherapy, resulting in overall low therapeutic response for TNBC patients. Here we aimed to identify patterns of expression in responders vs non-responders by examining the signaling profile of metastatic (met) TNBC patients following targeted therapy against the PAM pathway. Ten patients were given an investigational oral combination of TAK-117 and TAK-228 (PIKTOR), a selective PI3Kα inhibitor and a TORC1/2 inhibitor respectively, predicted

to impair DNA damage repair (DDR) pathways, increasing genomic instability and tumor sensitivity to chemotherapy. The hypothesis was successful inhibition of the PAM pathway by PIKTOR could downregulate effectors/modulator proteins of NHEJ in HRD cells. Signaling profile of pre- and post-tumor biopsy samples following PIKTOR were mapped via RPPA. Overall analysis showed heterogeneity of disease and response to treatment. The proteomic profile indicated compensatory signaling in response to treatment via upregulation of partnering MAPK pathway or upstream RTKs. Heterogenous signaling in DDR signaling pathway suggest a nonspecific stress response by TNBC tumors, unlikely to correlate DDR deficiency to patient treatment response. Pathway expression analysis of metTNBC patients at baseline and post-PIKTOR therapy highlighted key nodes in the pathway which have the potential to contribute to disease relapse. Data generated from this study could elucidate common pathway of resistance accessible for future treatments and help guide future therapeutic discoveries for advanced, metTNBC.

INTRODUCTION

In 2017, approximately 260,000 new cases of breast cancer (BC) were diagnosed in the United States (*1*). The reported lifetime risk of developing BC is 12.4% for American women (*1*). Morphological characteristics divide BC into preinvasive carcinoma or invasive (infiltrating) carcinoma, with ductal carcinoma in situ (DCIS) and infiltrating ductal carcinoma (IDC) representing the most common subtype in each category respectively (*2*).

The 3 markers differentiating different types of BC are estrogen (ER), progesterone (PR) and HER2/neu receptor expression. Supplemental biomarkers such as Ki-67, VEGF, CK5/6, and EGFR might also be utilized to guide therapeutic treatments (*3*). Gene expression profile further divides BC into its intrinsic subtype of luminal A, luminal B, HER-2 enriched, basal-like (BL) or normal-breast-like (*4*). Of note, the most aggressive subtype is BLBC, more specifically triple negative breast cancer (TNBC) which makes up 80% of BLBC following Pam50 subtyping (*3*).

TNBC are deficient in ER, PR, and HER2/neu receptors (*3*). It accounts for approximately 15% of all invasive BC (*5*). Disease susceptibility is higher in younger women, women of African descent, and those with underlying germline mutations such as mutated *BRCA1* (*1, 6*). A cohort study on TNBC patients reported shorter progression free survival (PFS) and an overall shorter median time to death compared to other BC

subtypes (4.2 years vs 6 years) (*7*). Diagnosed patients tended to have higher reported mean tumor sizes, grade, node status and rate of metastasis to visceral organs (*5, 7, 8*). The reported 5-year survival from 2010-2016 for metastatic (met) TNBC patients was 12% (*6, 9*)

Poor outcomes in TNBC can be attributed to a combination of reasons, from late stage diagnosis, challenges in targeted therapy, and/or high mutational burden of TNBC (*3, 4, 10*). High inter- and intra- heterogeneity of TNBC can manifest as heterogeneous clinical manifestation, response, and pathology (*5, 11*). Attempts have been made to characterize the subtypes of TNBC, 6 subtypes were formulated from gene expression analysis: basal-like 1(BL1), BL2, mesenchymal (MES), MES stem-like, immunomodulatory, and luminal androgen receptor-AR (LAR) (*8*). These subtypes have not been able to predict therapeutic outcomes.

Pathologically high-grade BC often display loss of heterozygosity and/or abnormal expression of *ATM*, *BRCA*, and *TP53* (*3, 12*). BRCA1/2 are tumor-suppressor proteins that maintain DNA integrity and genomic stability by mediating double strand break (DSB) repair through homologous recombination (HR). Additionally, they also regulate genes involved in DNA repair, cell cycle and apoptosis (*13*). The histological and transcriptional profiles of TNBC are similar to *BRCA*-linked BC, where the triple negative phenotype is expressed in approximately 70% of BC occurring in *BRCA1* carriers, while this number diminishes to 23% in *BRCA2* carriers (*3, 14*). BRCAness or the inactivation of *BRCA* genes through somatic, germline or secondary means makes the

tumor more susceptible to mutations and more reliant on other pathways for double strand DNA repair (*15, 16*)

DSB repair is achieved through 2 main pathways, non-homologous end joining (NHEJ) or HR. The repair process follows a general scheme of DNA damage, damage detection, and recruitment of signaling/mediator and effector proteins. Main variations between the 2 pathways are error rates, key modulators, degree of end resection, and frequency throughout the cell cycle (*17*). HR is template dependent, has the highest fidelity and most active during the S and G2 phase (*16, 18*). The main effectors of this pathway are BRCA1/2, Rad51 and Rad54. On the other hand, NHEJ is template independent, more error prone, and dominant throughout the cell cycle due to the high levels of Ku proteins and its suppression of extensive end resection (*16, 17*).

NHEJ pathways are divided into classical (C) and alternative (A) pathways. C-NHEJ is regulated by heterodimers of Ku70-Ku80, DNA-PK complexes, polymerase, and nuclease complexes (*17*). Direct ligation by C-NHEJ is more precise than its counterpart, A-NHEJ or M-NHEJ which utilizes microhomologies, exposed via endonuclease activity, distant from the DSB. Modification of annealed intermediates and end structures are mediated by polymerases and ligases such as Pol θ and XRCC1 respectively (*19*). As this pathway necessitates degradation of DNA segments, A-NHEJ can contribute to genomic deletion, chromosomal translocation and/or mutations (*17*).

The antagonistic relationship between pro-HR and pro-NHEJ factors, balances which processes will be utilized for DSB repairs and when. These factors can include the availability of the sister chromatid template, active CDKs, and/or the presence of certain

proteins like 53BP1 (*15*, *17*, *19*, *20*). A-NHEJ is often utilized when C-NHEJ is inhibited and/or disrupted. Likewise, this pathway can function as a backup for HR deficient (HRD) cells due to the shared mechanism utilized by the 2 processes. High proportions of BLBC are characterized by HRD (*14*, *21*). HRD can occur through BRCA1/2 mutation, methylation/silencing of *Fanconi Anemia* (*FA*) genes (*22*), loss of CDK1 activity (*23*) , loss of Rad51-dependent foci formation (*24*), *TP53* mutation (*4*), and/or PI3K inhibition (*25*).

Tumors without *BRCA* impairment frequently have *PIK3CA* mutation (*4*, *26*). The PI3K/AKT/mTOR (PAM) signaling pathway plays a key role in regulating motility, metabolism, cell proliferation, migration, and survival of TNBC (*26*). Aberrant activation of this pathway has been shown to drive malignant transformation and induce resistance to chemotherapy. The Cancer Genome Atlas (TGCA) network reported *TP53* (74%) to be the most mutated gene overall, followed by *PIK3CA* (18%) encoding PI3Kα in TNBC. The prevalence of *TP53* mutation is higher in BL TNBC while *PIK3CA* mutation occurs more frequently in LAR TNBC (*26*). PTEN and INPP4B phosphatases, negative regulators of PI3K, are more commonly inactivated in BL TNBC and LAR TNBC respectively. Incidences of *PTEN* mutation/loss of expression, genomic loss of *INPP4B* and *PIK3CA* overexpression are higher in TNBC than other BC types (*27*, *28*).

Monotherapy and combination clinical trials targeting pan-PI3K, isoform specific PI3K, mTORC1/2, and dual PI3K/mTOR are ongoing with the goal of increasing overall survival from gold standard, neoadjuvant chemotherapy. Chemotherapy is efficacious because of the vulnerable state induced by extensive genomic instability and deficient

DNA damage repair mechanism in TNBC (*3*, *4*, *6*). However, there is high degree of systemic relapse with conventional therapy. The paradox of higher response to chemotherapy is countered with the increased risk of recurrence (*5*). Combination of chemotherapy plus dual molecular inhibitors have the best reported overall improvement in patient response. Unfortunately, all new drugs have failed to be validated in phase 3 trials (*29*).

PIKTOR was a phase II clinical trial that aimed to improve patient response by fully inhibiting the PAM signaling pathway, while taking advantage of the intrinsic genomic instability in TNBC patients as a result of DDRD. The trial utilized a combination of TAK-117, a selective PI3Kα inhibitor (*30*), and TAK-228/Sapanisertib, a TORC1/2 inhibitor (*31*), to silence the key modulators and sensitize/prime the metastatic tumors. Priming the tumor was predicted to make the tumor more susceptibility to chemotherapy and improve overall patient response (*32*).

The goal of this project was to examine the signaling profile of patient biopsy samples at baseline/before PIKTOR and after PIKTOR treatment via laser capture microdissection, reverse phase protein microarray technology, and immunostaining. The hypothesis was successful inhibition of the PAM pathway by PIKTOR could downregulate effectors/modulator proteins of NHEJ in HRD cells. Cellular signaling analysis before and after therapy indicated non-specific effects on DDR pathways and partial inhibition of the PAM pathway by PIKTOR. A trend of compensatory signaling in response to treatment inhibition was observed in the majority of patients. The finding from this project, in combination with findings from collaborators of the PIKTOR

project, can elucidated possible avenues of resistance to targeted PAM inhibition and improve future efforts in molecular targeted therapy against metTNBC.

METHODS

Enrolled patients (n=10) were women with a median age of 51 and had received 3 or more therapeutic treatments prior to PIKTOR. All patients received a combination of TAK-228 and TAK-117 until disease progression (PD), followed by cisplatin (cis) and nab-paclitaxel (nab-pac) for up to 6 cycles. The PIKTOR combinations were administered orally and cis+nab-pac administered intravenously every 3 weeks until PD. Post-treatment therapy following chemotherapy were pembrolizumab, eribulin, bevacizumab, and/or olaparib in different combinations.

Primary and secondary outcomes were assessed for the duration of the clinical trial. Objective response rate and the duration of the response associated with sequential treatment of PIKTOR followed by cis plus nab-pac were used for the assessment of therapeutic efficacy. Reverse phase protein array (RPPA) analyses were performed on pre-and post-PIKTOR tissues, where "pre-" implied baseline biopsy samples before the administration of PIKTOR, and "post-" being biopsy taken at PD but before chemotherapy.

Clinical Samples and Laser Capture Microdissection (LCM)

A total of 20 core biopsies representing pre and post PIKTOR treatment specimens were embedded in cryopreservative solution (OCT) and stored at -80℃. Frozen tissue sectioning (8μm) and manual LCM (PixCell system) were performed as previously described (*33*). A range of 35-50 slides were cut and stored at -80℃ for each sample with 1-2 slides reserved for hematoxylin-eosin (H&E) staining. Tumor and

stroma areas were identified on H&E slides prior to LCM. Dissection efficiency was much higher for the stroma sections compared to the tumor section on the same tissue. Dissected tissue were lysed with a solution of 10% (v/v) Tris(2-carboxyethyl)phosphine (TCEP; Pierce) in 45% (v/v) Tissue Protein Extraction Reagent (T-PERTM, Pierce) and 45% (v/v) Tris-glycine 2X SDS buffer (Invitrogen). The combined lysates for each core set, divided by stroma/tumor/heterogeneous whole cell, were heated at 70℃ for 5 mins and stored at -80℃ prior to microarray construction.

Reverse Phase Protein Array (RPPA)

Individual lysates (250µg/mL) and 2-fold (8 point) dilution curves of the 3 control lysates were loaded into a 384 well plate. The lysates were printed in duplicates onto glass backed nitrocellulose array slides (Grace BioLabs, Oncyte Avid) using an Aushon 2470 arrayer (Aushon BioSystems) equipped with 350 mm pins as previously described (*34*). BSA (1mg/mL) (ThermoFisher, cat. 23209), MCF7 + EGF + β-estradiol (0.5mg/mL) (SantaCruz Biotechnology, cat. SC24730), SK-BR-3 (0.5mg/mL) (SantaCruz Biotechnology, cat. SC2134), and BT474 (lab brew) served as positive control. Lysis buffer alone was printed to account for any contaminations in the buffer. Total protein values were assessed with Sypro Ruby Blot Stain (Invitrogen/Molecular Probes) per manufacturer's directions. The slides were stored in desiccant at -20℃ prior to immunostaining.

Immunostaining

The arrays were treated with 1X Reblot (Chemicon, cat2502) for 15 minutes, followed by 2, 1X PBS wash for 5 minutes each, and blocked in I-Block (Applied

biosystems, cat. T2015; 1X PBS and .1% Tween 20) for 1 hour. Immunostaining was performed as previously described (*35*) on a Dako Autostainer per manufacturer's instructions (CSA kit, Dako cat. K1500). Polyclonal and monoclonal antibodies utilized in the study are listed in Table 1. All primary antibodies with their corresponding secondary were validated for specificity by Western blots as previously described (*36*). Slides were incubated with either goat anti-rabbit IgG H+L (1:10,000) (Vector Labs, cat. BA-1000) or anti-mouse IgG HRP (1:10) (Dako, cat. K1500). Secondary alone served as a negative control. Signal detection and amplification was achieved through the addition of streptavidin-biotin complex (SABC), amplification reagent (biotinyl tyramide), streptavidin-HRP, and diaminobenzidine (DAB), with rinsing and auxiliary washes in between each step.

Each array was scanned on a standard flatbed scanner (UMAX) with Adobe Photoshop at 14bit images/600dpi for analysis. Spot intensity from the scanned images were quantitated and adjusted for background correction using ImageQuant ver5.2 (Molecular Dynamic). Protein values were normalized using RPMA_Analysis_Suite_01_15. Final normalized signal intensities were incorporated into JMP 5.0 software (SAS), and unsupervised hierarchical clustering analysis was performed as previously described (*37*). Wilcoxon signed rank test paired the matched pre/post tissue and assigned significance (p-value) to all chosen endpoints. Mann Whitney U (MWU) testing was performed on unpaired, pre-stratified patient samples. Both tests were nonparametric and p-values ≤ 0.05 were considered significant. Log2

fold change (Log2FC) was calculated to represent the increase/decrease in protein expression.

Table 1: Validated primary antibodies for Reverse Phase Protein Microarray (RPPA) analysis

Antibody	**Vendor**	**Polyclonal/ monoclonal**	**Function**
53BP1	Cell Signaling Technology	Monoclonal	DNA Damage Response
AKT (Ser473)	Cell Signaling Technology	Polyclonal	Growth/Prosurvival
Androgen Receptor (AR)	Cell Signaling Technology	Monoclonal	Growth factor receptor
BRCA1	Cell Signaling Technology	Monoclonal	DNA Damage Response
BRCA2	Cell Signaling Technology	Monoclonal	DNA Damage Response
CD45	BD Transduction	Monoclonal	Immune recognition/response (B-cells + T-cells)
CDK2	Cell Signaling Technology	Monoclonal	Cell Cycle/ G1-S transition
Cleaved PARP (Asp214)	Cell Signaling Technology	Polyclonal	Apoptosis
DNA-PKcs	Novus Biological	Polyclonal	DNA Damage Response
EGFR (Thr654)	Invitrogen	Monoclonal	Growth factor receptor
EGFR (Tyr1173)	Invitrogen	Polyclonal	Growth factor receptor
ErbB2/HER2 (Tyr1248)	Cell Signaling Technology	Polyclonal	Growth factor receptor
ErbB3/HER3 (Tyr1289) (21D3)	Cell Signaling Technology	Monoclonal	Growth factor receptor
ERK1/2 (Thr202/Tyr204)	Cell Signaling Technology	Polyclonal	Growth/Prosurvival
FOXO1/ FOXO3 (Thr24/Thr32)	Cell Signaling Technology	Polyclonal	Cycle cell arrest/Apoptosis
Histone H2AX (Ser139)	Cell Signaling Technology	Monoclonal	DNA Damage Response

IGF1Rb (Tyr1131), INSRb (Tyr1146)	Cell Signaling Technology	Polyclonal	Growth factor receptor
IGF1Rb (Tyr1135), INSRb (Tyr1136)	Cell Signaling Technology	Polyclonal	Growth factor receptor
Ku80	Cell Signaling Technology	Monoclonal	DNA Damage Response
LC3B	Cell Signaling Technology	Polyclonal	Autophagy
MEK1/2 (Ser217/Ser22)	Cell Signaling Technology	Polyclonal	Growth/Prosurvival
mTOR (Ser2448)	Cell Signaling Technology	Polyclonal	Growth/Prosurvival
Neutrophil Elastase	Abcam	Polyclonal	Immune response
NRF2	Cell Signaling Technology	Monoclonal	Antioxidant response
p70 S6K (Thr389)	Cell Signaling Technology	Polyclonal	Growth/Prosurvival
PDL1	Cell Signaling Technology	Monoclonal	Immune Response/ Programmed cell death ligand
PI3K p110y	Cell Signaling Technology	Polyclonal	Growth/Prosurvival
pS6RP (Ser235/Ser236)	Cell Signaling Technology	Monoclonal	Growth/Prosurvival
Rad51	Cell Signaling Technology	Monoclonal	DNA Damage Response
Rad54	Cell Signaling Technology	Monoclonal	DNA Damage Response
RASGRF1 (Ser916)	Cell Signaling Technology	Polyclonal	Growth/Prosurvival
SAPK/JNK (Thr183/Tyr185)	Cell Signaling Technology	Polyclonal	Growth/Prosurvival

RESULTS

Patient Response

Ten patients received the combination of PIKTOR followed by cisplatin (cis) plus nab-paclitaxel (nab-pac) (Tab. 2). The median prior chemotherapy regimen was 3, of which 7 patients received carboplatin. Sites of metastases included lymph nodes (n=8), lung (n=6), chest wall (n=1), bone (n=1), and brain (n=1). The median time on PIKTOR was 8 weeks. Patient response was divided between stable disease (SD=4) and progression of disease (PD = 6), where PD signified a reported PFS of $\leq$ 20 weeks after PIKTOR treatment. No patient experienced a complete response. Patient 1, 4, 8 and 10 experienced SD at the completion of PIKTOR. Patient 1 and 8 experienced the longest PFS of 49 weeks and 58 weeks, respectfully. Patients 1, 6, and 8 were classified "Responders" because they had durable SD for +14 months on pembrolizumab treatment, post cis/nab-pac. The priming combination of PIKTOR followed by cis/nab-pac did not produce durable response in most patients.

Table 2: Patient Demographic and Treatment. Ten patients received PIKTOR followed at progression by cis/nab pac. Baseline median number of prior chemotherapy regimen was 3 (range 1-5). Median time on PIKTOR prior to PD was 8 weeks (range 3-14). Post study treatment defined responder versus nonresponders, where responders experiences PFS > 60 weeks.

Patient		**Baseline Treatment**		**Treatment on Study**				**Post Study Treatment**	
Patient ID	**Site of Met. Disease**	**Total regimens prior to PIKTOR**	**# prior regimen in metastatic setting**	**Total weeks on PIKTOR**	**Duration on cis + nab-pac (weeks)**	**Response at study completion**	**Progression Free Survival (weeks)**	**Treatment (Pembrolizumab, others)**	**Duration (Weeks)**
1	LN, Bone, Brain	4	2	7	16	SD	65	Pembrolizumab, Olaparib	103
2	Chest wall, LN, Lung	3	0	9	3	PD	4	Eribulin	5
4	LN, Lung	2	0	10	17	PR	33	Paclitaxel + Bevacizumab + Pembrolizumab	18
5	LN, Lung	1	0	5	9	PD	13	Eribulin + Pembrolizumab	9
6	LN	3	3	11	6	PD	10	Pembrolizumab	69
8	LN	2	1	14	18	SD	76	Pembrolizumab	61
9	Lung	1	1	4	7	PD	14	Pembrolizumab	3
10	LN	2	1	14	17	SD	20	N/A	N/A
11	LN	4	3	7	3	PD	4	Paclitaxel + Bevacizumab + Pembrolizumab	2
12	LN, Lung	5	3	3	6	PD	8	Erubilin	6

Overall heterogenous signaling within the patient population showed the importance of LCM prepared samples.

Thirty-three total patient samples were analyzed for signaling pathway activation of 32 phospho-specific and total endogenous protein antibodies. The chosen epitopes were key signaling molecules regulating cell survival, growth, autophagy, stress response, DNA damage repair, and immune signaling. Unsupervised hierarchical clustering of protein expression status of all 33 samples across 32 endpoints (Fig. 1) revealed 4 major sample clusters, plus 1 outlier. There were no obvious trends of protein inhibition/overexpression in the 4 protein clusters or between patient samples. This observation was partially due to the conflicting signaling patterns of the combined tumor, stroma, and whole tissue samples.

Comparison of protein signaling profile in patient-matched lysate from LCM procured samples versus whole tissue lysate found no clear matched clustering. There was one direct matched cluster in patient 8 post-PIKTOR microdissected pure tumor and pre-PIKTOR whole tissue sample. If this was interpreted at face value, the signaling profile pre- and post-treatment would imply a lack of response to treatment as seen in the case of patient 12, but this was not the case for patient 8. The majority of patient samples showed significant divergent signaling profiles between the tumor/stroma/whole tissue samples from the same patient.

The distinct clustering patterns of the same pre-PIKTOR, whole tissue sample from patient 9 offers a great example (Fig. 1). In the first case, patient 9 pre-PIKTOR

sample displayed high expression of the first cluster of endpoints on the horizontal axis, separated from the rest of the patient sample. In the second case, the “same” sample showed low to medium-low expression of the same group of endpoints. Both samples were treated the same way, differing only in the time the tissue biopsy was received, but this factor does not have a significant impact because the samples were kept stable at -80℃. The variations between the signaling profile of pure LCM-procured and whole tissue samples, highlighted the importance of microdissecting tissue samples prior to RPPA.

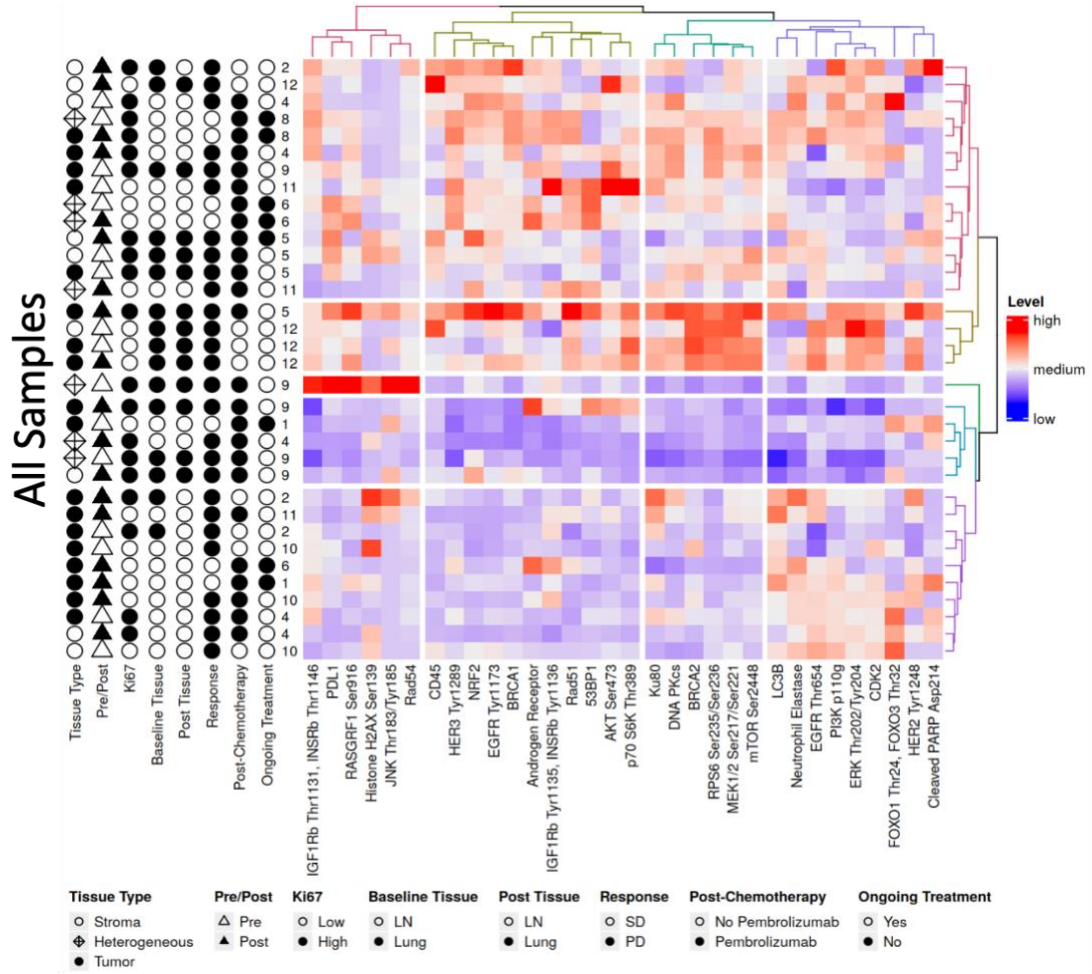

Figure 1 Unsupervised hierarchical clustering of 33 TNBC tissue samples analyzed by RPPA. Protein endpoints are represented in columns, samples in rows. Higher relative level of protein expression is represented in red, lower level in blue. Four computer generated clusters grouping the different signaling profile of all samples are categorized by pink, yellow, green, blue, and purple. The grouping of the clusters at each split on the dendrogram imply increasing similarity between the different samples. The identifier in the legend corresponds to the tissue type (stroma/tumor/heterogenous whole tissue); pre-PIKTOR or post-PIKTOR; High (>70%) or Low (<70%) Ki-67 levels measured pre-PIKTOR; Post biopsy site of either lymph nodes (LN) or Lung; Response post-PIKTOR as disease progressor (PD) or stable disease (SD); Treatment intervention post chemotherapy utilizing pembrolizumab or eribulin, bevacizumab, and/or Olaparib in different combinations; Ongoing treatment intervention post chemotherapy as continuing (yes) or discontinued (no).

The signaling noise generated by the stroma/microenvironment is likely to contaminate the true signaling within the tumor itself, which is commonly much smaller in magnitude. These confounding variables in the stroma could increase signaling

expression of the measured proteins, masking the true contribution from the tumor environment of interest, and skewing downstream analysis. As a result of the heterogeneity of the patient samples, and the risk of signaling noise when grouping samples based solely on patient identifiers, subsequent analysis was performed only on pure tumor samples acquired from LCM.

Clustering of tumor samples revealed 3 major outliers

Limiting the analysis to microdissected tumor samples (Fig 2) generated 4 patient sample clusters, two groups encompassed the majority of patients, while the other two groups zeroed in on the two greatest outliers within the patient population, patient 5 and patient 9. Patient 5 post-PIKTOR had elevated expression in 31 endpoints, the exception being EGFR (Thr654). Fold change of protein expression (Supplementary Table 2) showed a significant average 14-fold increase in cleaved-PARP (cl-PARP), FOXO 1/3 (Thr24/32), and AKT (Ser473) for patient 5. Genomic sequencing (Supplemental Table 1) of patient 5 identified wild type *BRCA1* (*BRCA1+*). Additionally, next gene sequencing (NGS) found a significant increase in copy number alterations (CNAs) post-PIKTOR treatment.

On the other hand, patient 9 genomic and proteomic profile showed a significant decrease after PIKTOR in CNAs, tumor mutational burden (TMB), and protein expression. Patient 9 experienced the greatest decrease in overall protein expression with only the exception of 53BP1, AR, Rad51, Rad54 and p70S6 (Thr389). The highest decrease in expression post-PIKTOR were of pS6 RP (Ser235/236) (40-fold), CDK2 (21-fold), and ERK1/2 (Tyr202/204) (38-fold). There were great similarities between patient

9 post-PIKTOR expression and patient 11 pre-PIKTOR expression (Fig 2). Protein expression (Supplementary Table 2) decrease in 15 out of 32 endpoints post-PIKTOR in patient 9 and patient 11. Interestingly, these two patients have very distinct clinical presentations.

Patient 11 was enrolled during stage 3 BC, had metastasis to the lymph nodes, and reported Ki-67 of 60%. This patient was heavily pretreated, with a total of 4 prior treatments overall, 3 in a metastatic setting (Table 2). Patient 9 however, was enrolled at stage 1 BC, had metastasis to the lungs, underwent 1 regimen prior to PIKTOR, and had a reported Ki-67 of 93%.

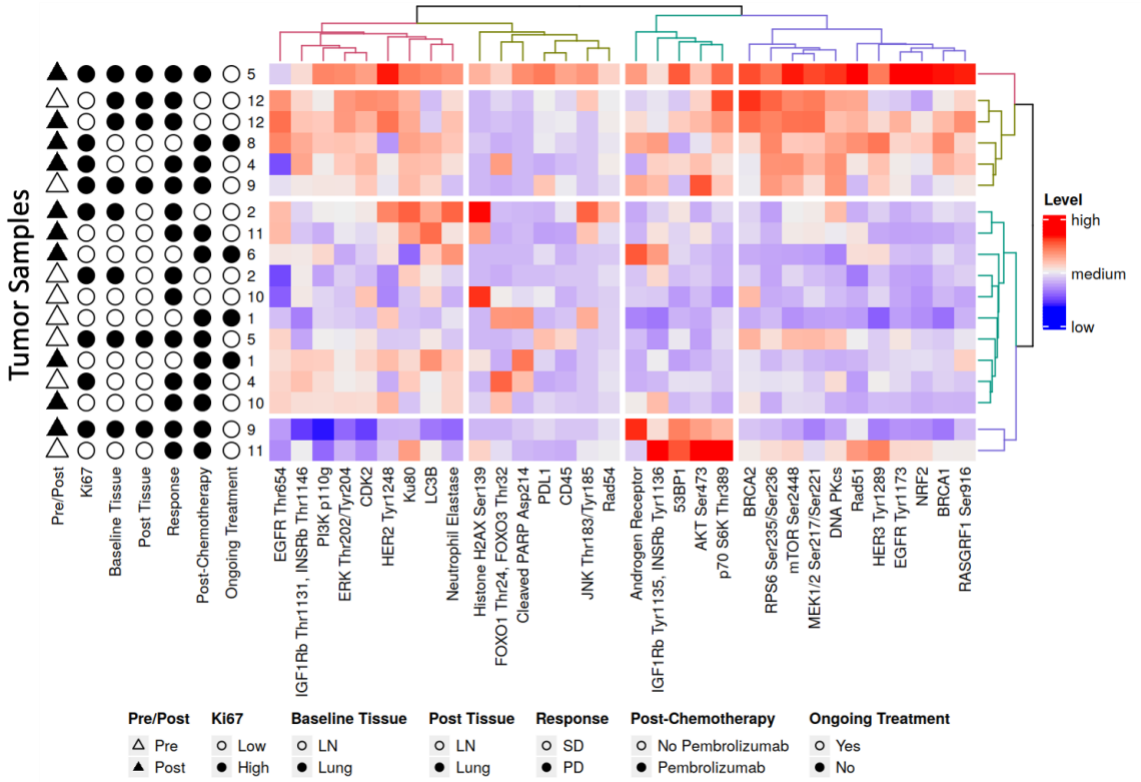

Figure 2 Unsupervised hierarchical clustering of LCM-procured tumor samples from TNBC tissue analyzed by RPPA. Heterogenous patient signaling. 4 groups of protein endpoints were identified via unsupervised hierarchical clustering utilizing the expression statues of 32 endpoints. Patient samples formed two main clusters represented the majority of the patients, while the other 2 clusters were made up of patient 5 post-PIKTOR tumor sample alone, or patient 9 post-PIKTOR and patient 11 pre-PIKTOR together. All identifiers in the legend and general dendrogram relationship is the same as Fig 1.

Patient 12 was the last outlier in this patient cohort, despite not experiencing a drastic increase/decrease in protein activation or clustering with patient 5 or patient 9. The decision to classify patient 12 as an outlier is due to the patient's unique matched expression pre- and post-PIKTOR, observed in the hierarchical cluster of all samples (Fig. 1), as well as tumor-only samples (Fig. 2). This lack of alternations in the proteomic profile of the endpoints chosen potentially indicated a very limited effect on the tumor population by PIKTOR. A common factor between patients 9, 11, and 12 were the rapid

time to disease progression on PIKTOR, where the total weeks on PIKTOR were 4 weeks, 7 weeks, and 3 weeks respectively (Table 2).

Compensatory upregulation of upstream receptor tyrosine kinases (RTKs) and the mitogen activated protein kinase (MAPK) pathway is indicated in the protein expression trend as a response to PIKTOR in the majority of metTNBC patients.

Next, we were interested in identifying the significant changes in key protein activation/inactivation status in response to PIKTOR. Wilcoxon paired testing of pre-PIKTOR vs post-PIKTOR tumor samples (Supplemental Table 3) were performed with the exclusion of patient 6 and 8 because both lacked a matched pre-PIKTOR tumor sample. The assumption in this case was that treatment is the main force contributing to the difference, irrespective of the site of tissue sample origin. No significant difference between pre- and post-PIKTOR treatment was found for any protein endpoint measured. To determine possible trends within the data that may highlight protein endpoints for further analysis we then evaluated statistical significance without multiple comparisons correction. An increase in HER2 (Tyr1248) phosphorylation ($p < 0.05$) and Rad54 expression ($p < 0.1$) were found following PIKTOR treatment.

Further statistical analysis was performed, with the exclusion of patient 9 (Supplemental Table 4) as an outlier in the data, as indicated by the clustering patterns. Again, no endpoint showed significant change between pre- and post-PIKTOR treatment. Only when multiple comparisons correction was not applied did ten protein endpoints, in addition to HER2 (Tyr1248), change expression or phosphorylation following PIKTOR treatment ($p < 0.1$). These proteins included PI3K p110γ, MEK1/2 (Ser217/221) and

ERK1/2 (Tyr202/204), LC3B, neutrophil elastase ($p<0.05$); mTOR (Ser2448), Ras GFR1 (Ser916), CDK2, and Ku80 ($p < 0.1$).

Protein expression analysis of pre-PIKTOR and post-PIKTOR was unable to identify significant differences between SD vs PD patients. Hierarchical clustering of tumor samples identified 2 distinct responses in the SD group.

In addition to identifying the differences in protein expression before and after treatment, statistical analysis utilizing unpaired MWU testing focused on pre-stratified patient samples based on their Ki-67, *PTEN* status and response to PIKTOR, as either SD or PD (Table 1). The SD group were patients 1, 4, 8 and 10, and PD group were patients 2, 5, 6, 9, 11, and 12. No significant differences between the endpoints from the PD vs SD groups were found in the pre-PIKTOR or post-PIKTOR tumor samples (Supplemental 5). Only when multiple comparisons correction was not applied did the mean pre-PIKTOR expression of Ras-GFR1 (Ser916) in the PD group was higher than that of the SD group ($p < 0.05$). Under the same condition, the SD group mean FOXO1/3 (Thr24/32) and cl-PARP expression was high than PD ($p < 0.05$). There were no correlations between Ki-67 levels measured prior to treatment and treatment response. *PTEN* alterations pre-PIKTOR were identified in patient 9 (mutation), patient 4 and patient 10 (deletion); statistical testing utilizing this criterion did not show any significant difference between altered and wild type.

Combined tumor sample clustering (Fig 2) of all endpoints found similarities in signaling between patient 8 post-PIKTOR and patient 4 post-PIKTOR, although not exact. The greatest anomaly in patient 4 was the 35-fold decrease in EGFR T654

expression (Fig 3). Among all classified SD patients, post-PIKTOR expression between patient 1 and 10 showed the highest degree of similarities. It should be noted that patient 10 post-PIKTOR expression is more similar to the expression of patient 4 pre-PIKTOR, but the clustering pattern of patients 1 and 10 are close enough to provide an estimate. This estimation played into the matched cluster of patients 1 and 10 in the designated mapping of PAM signaling, receptor kinase signaling, and DDR signaling.

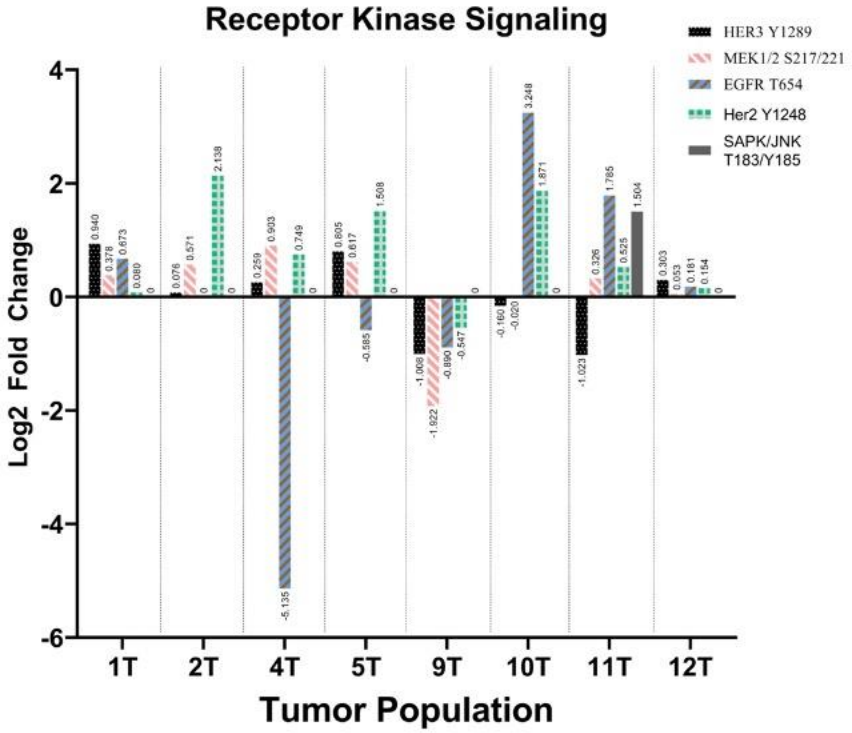

Figure 3: Log2 fold change receptor kinase protein expression pre- and post- PIKTOR with the exclusion of patient 6 and 8. HER2/3, EGFR T654, MEK ½, SAPK/JNK was included based on the string network analysis. 35-fold decrease of EGFR-T654 in patient 4. Overall decreased expression in patient 9.

PI3K/AKT/mTOR Pathway was partially inhibited by PIKTOR.

Next, we focused our analysis on key nodes of the PAM pathway. Hierarchical clustering of key nodes within the PAM pathway encompassed the 5 key proteins, PI3K

p110γ, AKT (Ser473), mTOR (Ser2448), p70 S6K (Thr389), and pS6 RP (Ser235/236). Similar expressions were identified between AKT (Ser473) and p70 S6K (Thr389), as well as mTOR (Ser2448) and pS6 RP (Ser235/236) (Fig. 4A). Log2FC expression (Fig 4B) points to an increase in the expression of all key proteins with the exception of pS6 RP (Ser235/236), for the majority of patients.

The SD group was divided between high expression post-PIKTOR (patient 4 and patient 8) and low expression post-PIKTOR (patient 1 and 10), as predicted from the tumor sample clustering (Fig 2). PI3K p110γ expression was the only common denominator between the 2 groups. Overall, there were 2 main clusters dividing all patients between low and high PAM pathway expression. There was a divergence of PI3K p110γ signaling from the rest of its downstream effectors AKT (Ser473), mTOR (Ser2448), pS6 (Fig 1 and Fig 4A). Due to the non-specific response and heterogenous signaling presentation, it was hypothesized that the PAM pathway might only be partially inhibited by PIKTOR.

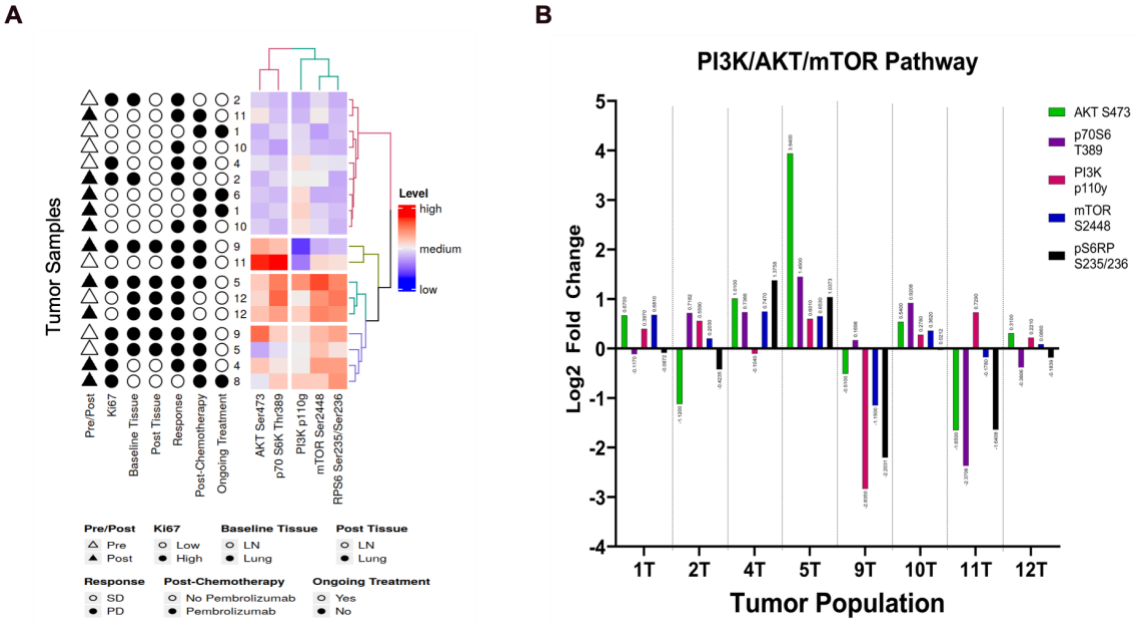

Figure 4: PI3K/AKT/mTOR pathway protein expression in tumor samples. Patients are grouped based on similar signaling profiles between tumor samples acquired from baseline/pre-PIKTOR biopsy or disease progressed post-PIKTOR. **(A) unsupervised hierarchical clustering of PI3K/AKT/mTOR pathway proteins from LCM-procured tumor samples of TNBC tissue analyzed by RPPA.** The groups are divided into 3 clusters, patient 9 post-PIKTOR and 11 pre-PIKTOR following the trend of the parent heatmap, cluster separately from the rest of the patient samples. All identifiers in the legend and general dendrogram relationship is the same as Fig 1. **(B) Log2 fold change of protein expression pre- and post-PIKTOR with the exclusion of patient 6 and 8.** Patient 1, 2, 11, 9 and 12 showed a decrease in pS6 RP (Ser235/236).

PIKTOR treatment did not inhibit DNA damage response in the majority of patients.

The status of HR and NHEJ was evaluated by analyzing the expression of DDR proteins post-PIKTOR in tumor samples. DDR pathway expression mapping directly assesses the HR pathway via BRCA1, BRCA2, Rad51, Rad54 expression, while Ku80, DNA-PKcs, 53BP1 reflects activation/inactivation of NHEJ. Unsupervised hierarchical clustering (Fig 5A) revealed post-PIKTOR patient cluster of patients 6 and 9; patients 1 and 10; patients 2 and 11. A cluster of patients 6 and 9 only appeared in the DDR signaling pathway. Endogenous androgen receptor (AR) expression between these 2

patients was the highest relative to all the other patient samples. Beside the *BRCA1*-statues, patient 6 and patient 9 had very little observable similarities in the available clinical, genomic, and proteomic profile.

Patient 1 and 10 expression post-PIKTOR had the greatest similarities out of the 3 patient clusters. There was low to medium-low expression in all 10 designated end points except CDK2 (Fig 5A). Despite baring such resemblance at the end of PIKTOR, patients 1 and 10 underwent opposite paths, over different periods of time to reach the final expression profile. Patient 1 was on PIKTOR for 7 weeks, experienced a high increase in CNAs and Log2FC (Fig. 5B) of DDR pathway protein expression from pre-PIKTOR to post-PIKTOR. On the other hand, patient 10 was on PIKTOR for 14 weeks, pre-post biopsy analysis showed a decrease in CNAs and corresponding decrease in Log2FC of DDR pathway protein from pre to post-PIKTOR.

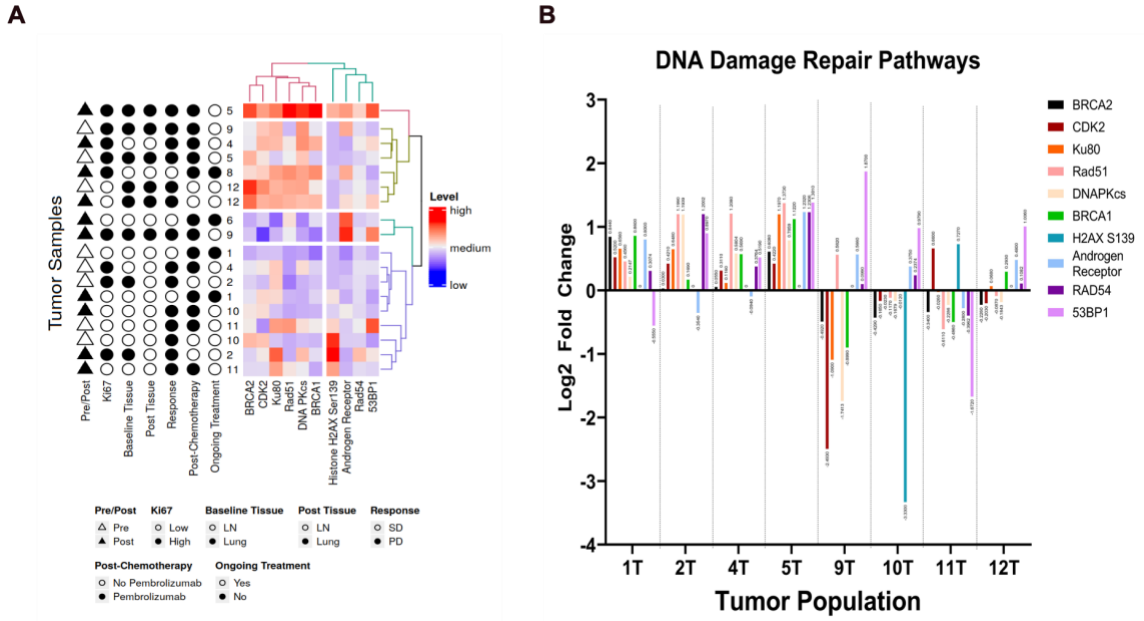

Figure 5: DNA Damage Repair (DDR) pathway protein expression in tumor samples. Double strand break repair utilizes homologous recombination assess via BRCA1/2, Rad51/54 expression, and nonhomologous end joining assess via 53BP1, DNA-PKcs, and Ku 80. **(A) Unsupervised hierarchical clustering of DDR pathway proteins from LCM-procured tumor samples.** Clustering pattern generated 4 main groups, the same observed in the parent heatmap. Patients 6 and 9 are in a separate cluster, separated by the low expression in all endpoints except Androgen Receptor (AR). Patient 2 and 11 at the bottom showed resemblance in signaling. All identifiers in the legend and general dendrogram relationship is the same as Fig 1. **(B) Log2 fold change of protein expression pre- and post-PIKTOR with the exclusion of patient 6 and 8.** Patient 9, 10 and 11 experienced decreases in expression, while the remaining five patients displayed an increase in expression.

Patient 2 and 11 protein expression post-PIKTOR matched their clinical characteristics and response. They both exhibited high expression of Ku80, LC3B, and H2AX. Patient 2 experienced a greater relative change post-PIKTOR, as compared to patient 11 whose signaling expression post-PIKTOR was closer to their expression pre-PIKTOR. Taking a closer look at the FC of protein expression from baseline for patient 2 (Fig 4B), there was an average 2-fold increase of Rad51, DNA-PKcs, Rad54 and 53BP1 expression. Genomic alteration analysis identified a *BRCA1* mutation, increased TMB and CNAs following analysis of pre-post biopsy samples of patient 2. The inverse

BRCA1+ status, and decrease in TMB and CNAs were identified in patient 11. NGS whole exome sequencing and subsequent single nucleotide variants analysis of patient 2 biopsy sample also identified an amplification of UVRAG, a gene involved in autophagic response to UV radiation.

These three clusters displayed shared resemblances within each group that could provide some contextual clues in terms of patient response at the stop of PIKTOR, but there was no consensus supporting the hypothesized decrease in DDRD trend as a result of PIKTOR. The signaling pattern of DDR pathway is once again very heterogenous. There were no pattens of downregulation in HR, NHEJ or both in the majority of patients samples post-PIKTOR. On the genomic side, NGS analysis did not identify HRD markers to be predominantly expressed in the pre- or post-PIKTOR biopsies. APOBEC (cytidine deaminase) and DNA mismatch repair (MMR) signatures were observed at a higher frequency in the majority of patients, with the exception of patient 10 and 11. *TP53* alterations (mutation/deletion) were observed in all patients. Therefore, it could be proposed that PIKTOR did not successful increase DDRD as intended.

Evasion of immune-mediated response influence the response to Pembrolizumab.

The only long-term responder not included in the SD group following PIKTOR was patient 6. Patient 6 was analyzed under the lens of a patient who did not benefit from targeted PAM therapy and chemotherapy but benefited from immunotherapy. In terms of PAM signaling post PIKTOR in the tumor samples, patient 6 shared the characteristics seen in patient 1 and 10 (Fig. 4A). Despite only experiencing 10 weeks PFS, treatment

with pembrolizumab reversed the growth of the tumor and sustained the patient with a 68-week post-treatment duration.

All three responders experienced metastasis to the lymph nodes. Common denominator, in terms of protein expression, between patient 1,6, and 8 was the decrease in CD45 expression (Fig 2.), and the high to medium high expression of neutrophil elastase in following PIKTOR treatment. Concurrently, *TOX* gene, related to T-cell development and PD-1 expression is differentially overexpressed in pre-PIKTOR biopsies of the three responder patients. These factors could indicate a host immune response to the tumor that might have been suppressed via receptor-mediated interactions.

DISCUSSION AND CONCLUSION

The goal of this project was to examine the signaling profile of metTNBC patients, identify patterns of expression in responder versus non-responders, and gain an understanding of the signaling network of these patients in-vivo. The combinatory effect of PIKTOR followed by cisplatin (cis) plus nab-paclitaxel (nab-pac) produced a 4:6 PD:SD ratio. Overall RPPA analysis showed heterogeneity of disease and response to treatment. Protein expressions change between pre-PIKTOR and post-PIKTOR indicated compensatory signaling that could lead to treatment resistance. Heterogeneous response combined with the protein signaling profile before and after PIKTOR alluded to a partial inhibition of the PAM pathway and insignificant increase in DDR following PIKTOR treatment.

Frequent alteration of the PAM signaling pathway in TNBC patients and its key role in growth and survival, makes it a promising target for advanced TNBC patients. Unfortunately, this pathway experience high degree of interactions, crosstalk and feedback mechanisms built in to ensure quintessential processes of cellular life and survival are maintained (*38*). Increased expression of key nodes in the PAM pathway, and upstream RTK in response to the inhibitory drugs is an adaptive response characteristic of compensatory behavior. Either single or dual inhibition of PI3K, AKT or mTOR, can result in an upregulation of the MAPK pathway (*39*) or RTK (*40*). This phenomenon was observed in all patients except patient 9. In our study, resistance to PIKTOR is speculated to occurred either through the upregulation of phosphorylated

HER2, HER3, MEK1/2 and/or ERK1/2. Increased expression of growth and proliferation proteins in response to PAM pathway inhibition likely contributed to the lack of response from patients within the trial. The caveat is the lack of true significance in the change of protein expression following PIKTOR.

The divergence of PI3K p110γ signaling from the rest of its downstream effectors AKT, mTOR, pS6 needs to be interpreted with caution. Class I PI3K consists of 2 subclasses, IA and IB. Class IA PI3K are heterodimers of a p110 catalytic subunit and a p85 regulatory subunit, consisting of p110α, p110β, and p110δ isoforms (*27*). Class IB PI3Ks are heterodimers of the measured p110γ catalytic subunit. p110α, p110β isoforms are ubiquitously expressed, while p110δ and p110γ are restricted to leukocytes or the vascular system. It has been reported that in neoplastic cells harboring high levels of genomic instability isoform selectivity could be transient. Existing feedback mechanisms can activate class I enzymes following the targeted inhibition of a specific isoform (*28*). Therefore, the measured PI3K p110γ level cannot quantify the degree of PI3K inhibition by TAK-117, but can be interpreted as response mechanism following inhibition.

It has been reported that *BRCA1* mutation (*BRCA1*-) is correlated with DDRD (*14*, *15*). Applying this assumption to patient 5 with a *BRCA*1+ genotype, the stress induced from PIKTOR inhibition likely increased PAM signaling and DDR response. This increase potentially made patient 5 slightly more susceptible to chemotherapy, as indicated by a PFS of 14 weeks. Unfortunately, resistance quickly followed as the increase in protein signaling in pro-survival and DDR pathways likely found a way to bypass and resist treatment.

In the case of patient 2 and patient 6, *BRCA1* mutation could have made the tumor more susceptible to initial PAM inhibition because of the increased dependency on pro-survival pathways with HRD status. Patient 2 DDR signaling profile post-PIKTOR resembled patient 11 DDR signaling pre-PITKOR. However, patient 11 is *BRCA1+*, alluding to an increase in DDR to a proficient level. Genomic and proteomic alterations of patient 2 also indicates a reliance on autophagy for survival. As for patient 6, in addition to *BRCA1* mutation, an *AR+* genotype in LAR subtypes have been reported to increase reliance on *PIK3CA* overexpression (*8*, *41*). The susceptibility to PAM inhibition is shown in the 11 total weeks on PIKTOR.

AR has been reported to activate *PTEN* transcription in breast cancer cells (*41*). The increased expression of AR is only observed in patient 5,6, 8 and 9. The increase in AR along with 53BP1, Rad51, Rad54 and p70S6 (Thr389) in patient 9 paints a narrative of an upregulation of pro-survival pathways as supplemented by AR growth factor signaling. TNBC patients experience activation of estrogen signaling pathways in the absence of ER (*42*). The increased expression of 53BP1, Rad54 and Rad51 then could be residual of an attempt by the cell to repair its DNA in a nontraditional way.

53BP1 is a binding partner of p53, a chromatin remodeler and a positive regulator of NHEJ (*17*). The 53BP1/RIF1 complexs can prevent extensive end resection and block localization of BRCA1/CtIP at DSB sites in G1 phase. Decreased expression of 53BP1 in all responders (patient 1, 6 and 8) plus patient 11 could indicate a decrease/inhibition in NHEJ as previously predicted. The rebuttal to this claim is the ability of BRCA1/CtIP complexes to displace 53BP1/RIF1 to initiate HR. Degrees of HR deficiency based on the

mutation signature associated with *BRCA1* and *BRCA2* mutations needs to be quantified in order to properly assess the inhibition of NHEJ in these patients. If HRD is high, the tumor is more likely to default to NHEJ, which places a greater significance on the decreased activity of NHEJ.

All three responders were heavily pretreated with different regimens in combination with taxanes. Synergistic effects of TAK-228 and TAK-117 at their respective IC50 have been shown to reduce pathway activation, activate autophagy and induce cell cycle arrest (*43*). Evidently, successful inhibition of the PAM pathway following selective inhibition of PI3Kα and mTORC1/mTORC2 potentially re-sensitized the tumor to taxane therapies like paclitaxel. A possible reasoning for the response of patient 8 to PIKTOR was the stressed induced upregulation of pro-survival pathways forcing the tumor to become more dependent on the PAM pathway signaling for survival, which then sensitized the tumor to cis + nab-pac.

The expression levels were high for the targeted PAM pathway proteins in patient 8 tumor samples post-PIKTOR. The difference in signaling between patient 8 and patient 4 provided a story of decreased G1/S cell cycle activity and 53BP1. By looking at only these 2 endpoints alone, it could indicate impairment of DDR pathways. However, this would ignore BRCA1/2, Rad51, Rad54, DNA-PKcs expression, which also regulate DDR pathways. A decrease in CDK2 was also observed but whether it was directly caused by PIKTOR therapy is unknown.

Patient 1 pre-PIKTOR PAM pathway signaling clustered with the signaling profile of patient 10 pre-PIKTOR. Both patients exhibited low levels of expression before

PIKTOR, but patient 1 progressed after 7 weeks and patient 10 progressed after 14 weeks. The low expression could be interpreted as a limited dependency on the PAM pathway itself or the canonical signaling of the PAM pathway. The difference that separate patient 1, a durable responder of 65 weeks before immunotherapy, from patient 10, a stable patient for 20 weeks before immunotherapy, in terms of their pathway activations and resistant mechanism warrant further studies. I suspect a different underlying reasoning for the final durable response of patient 1 that could be unrelated to PIKTOR inhibition as far as the data is concern.

As for the durable response of all 3 patients following pembrolizumab, factors such as the overexpression of PD-1 in dysregulated PAM pathway (*44*), upregulation of PD-L1 in PTEN mutations(*45*), and/or increased presence of tumor infiltrating lymphocytes (TILs) (*46*) could positively influence patient response to therapy. The DDR pathway expression of patient 6 after PIKTOR showed high degrees of similarity with patient 9 post-PITKOR, therefore it is safe to assume that DDR pathway disruption was not the main causative explanation for patient 6 response in this trial. Additionally, due to the similarities in PAM signaling shared by patient 1, 6, and 10 post PIKTOR, it further questions the effect of PIKTOR on therapeutic response.

There were a few limitations to this study in its approach and data interpretation. First, the lack of biomarkers for therapeutic resistance greatly influenced the percent of success in this phase 2 single arm clinical trial (*47*). Second, heterogeneity in patient samples in terms of preparation difference in NGS versus proteomic studies was a confounding variable for the final analysis. The NGS studies were performed on

heterogeneous samples, whereas the proteomic analysis was performed on microdissected tumor or stroma. Third, in a study involving patients with metastatic diseases, it is difficult to pinpoint how much each treatment/therapeutic compound contributed to overall therapeutic efficacy. Heavily pre-treated patients with metastatic disease makes it difficult to ascribe patient treatment response in a direct cause-effect manner.

Lastly, the small sample size limited the ability to properly account for the effect of differential signaling based on metastatic sites and made it more challenging to make inferences about the pro-survival mechanisms utilized in other TNBC patients with similar genetic alterations because of the heterogeneous nature of the disease. Pathway activation is heavily influenced by the underlying microenvironment of the metastatic site. Patient response to treatment analysis ignored the influence of the biopsy site because proper division of samples based on the metastasized regions (LN or Lung) was not possible with the limited patient sample. The effect of tumor microenvironment on the signaling cascade can be a confounding variable when the metastatic biopsies were taken from different sites in each patient (*48*). This might have concealed trends or significant expression differences that could have potentially be identified if there was sufficient data to make independent groups.

This project was a perfect example as to why personalized medicine is crucial and extremely vital in the war against cancer. Often, the clinical phenotype and manifestations cannot fully represent the interworking mechanisms driving resistance and disease progression. Patients 1 and 8 were the only 2 patients which benefited greatly from PIKTOR treatment. as indicated by their PFS of +1 year. Beside this fact, there was

nothing tying these patients together in the analysis performed. The clinical profile of these 2 patients also differed greatly in terms of Ki-67 levels, stage of BC, treatment regimens prior to PIKTOR and duration on PIKTOR.

In conclusion, advanced BC patients face limited therapeutic regimens that can increase their complete response (pCR) or progression free survival (PFS). The difficulty in finding adequate treatments for metTNBC is due to the lack of a targeted treatment (*49*), high clonal heterogeneity (*50*), and high probability of acquiring resistance. Pathway expression analysis of metTNBC patients at baseline and post targeted PIKTOR therapy highlighted key nodes in the pathway which can contribute to a lack of response. Future therapies in this population could incorporate AR and RTK inhibitors. High levels of AR have been shown to contribute to therapy resistance and stimulate cellular proliferation in TNBC (*51*, *52*). Combination treatment of PAM inhibitors and AR antagonists can reduce tumor growth and increase response in patients with high AR expression and PI3KCA mutations. Feedback loop activating upstream RTKs like epidermal growth factor receptor (EGFR) and Type I insulin-like growth factor receptor (IGF-IR) can be a promising target for combinatory inhibition because of the abundancy in TNBC patients (*53*) and natural response of the cell to increase expression to acquire resistance/survive. The increase in mutational burden and clonal heterogeneity adds additional factors to consider in the face of relapse and therapeutic resistance.

It might prove beneficial to adapt what has been shown to be effective for early stage TNBC in the hopes of mimicking the desirable effects, even if it is not to the same level. Tremendous work has gone into stratifying patients to provide the most effective

neoadjuvant treatment. Clinical trials such as I-SPY2 have shown great success in improving patient complete response in phase II trials (*49*, *54*). The I-SPY2 clinical trials are an adaptive trial that enroll early-stage BC patients with the hopes of improving their complete response (*55*). The interpretation and clinical trial development utilizing the data from the I-SPY2 trials will be performed with an understanding that metTNBC is more aggressive than its primary counterpart. Successful targeting of the PI3K/AKT/mTOR pathway has the potential to increase survival for most patients diagnosed with cancer. In the eyes of personalized medicine, there has been a push to classify cancer types not based on their primary or even metastatic sites but on their genotypic and phenotypic characteristics. The data generated from this phase II PIKTOR clinical trial could potentially help guide future therapeutics discoveries and testing.

APPENDIX 1

Supplemental Table 1: Patient Demographic and Genomic Alterations

Subject ID	Stage	Histological Grade	Genetics	Target lesions (sites of disease)
001	IIIA	3	BRCA1 +, PDL-1 -	Left internal mammary lymph node, aortic pulmonary window, SC fossa and mediastinum, anterior fifth rib, other abdominal LNs, brain
002	IIA	High grade	BRCA1 -, NGS -, p53 (clone D0-7 IVD) >90%, C110RF30 amplification, CDKN2A/B loss, TMB intermediate 6 mut	Left lateral chest wall, hilar and mediastinal lymph node, Lung
004	IIA	3	PD-L1 -, PTEN deletion	Right neck, mediastinum LN, superior border of right breast implant, lung
005	IIA	3	PD-L1 -	Right axilla LN, Lung
006	IIB	3	BRCA-1 -, AR + (7-8%), Guardant360 TP53 H179L and CDK4 amplification	Left internal mammary lymph node
008	IIB	3	PD-L1 +p53 80%	Left axillary, supraclavicular, thoracic and internal mammary LNs
009	IA	3	BRCA1 -, PD-L1 +, PTEN G36R, TP53, RB1 Q207	Right lung
010	IIIC	2	PD-L1 -, PTEN deletion	Supraclavicular, mediastinal and hilar LN
011	IIIC	3	BRCA1 +	Left supraclavicular LN
012	IIB	3	TP53, AURKA, PAK1, EGFR and MET overexpressed	1. Right partracheal LN 2.5x3.1 cm 2. +25 lung lesions largest 2.4 cm

APPENDIX 2

Supplemental Table 2: Fold Change Calculation of Protein (32 endpoints) Expression in Tumor Samples Before and After PIKTOR.

Sample ID	1Tumor	2Tumor	4Tumor	5Tumor	9Tumor	10Tumot	11Tumor	12Tumor
53BP1	0.681	1.862	1.433	2.604	3.656	1.971	0.314	2.008
AKT (Ser473)	1.590	0.460	2.018	15.349	0.702	1.455	0.319	1.244
Androgen Receptor (AR)	1.741	0.782	0.937	2.349	1.481	1.296	0.823	1.394
BRCA1	1.815	1.124	1.483	2.177	0.536	0.992	0.708	1.225
BRCA2	1.795	1.021	1.039	1.524	0.711	0.743	0.790	0.855
CD45	0.250	1.687	1.517	1.534	0.523	2.260	0.410	1.348
CDK2	1.433	1.339	1.241	1.340	0.178	0.892	1.580	0.869
Cleaved PARP (Asp214)	1.209	0.000	0.000	13.523	0.000	0.000	0.000	0.000
DNA-PKcs	1.160	2.288	1.495	1.724	0.299	0.890	0.853	0.880
EGFR (Thr654)	1.595	0.000	0.028	0.667	0.540	9.498	3.446	1.134
EGFR (Tyr1173)	1.484	1.088	1.155	2.395	0.523	1.149	0.547	1.673
ErbB2/HER2 (Tyr1248)	1.057	4.402	1.681	2.845	0.684	3.657	1.439	1.113
ErbB3/HER3 (Tyr1289) (21D3)	1.918	1.054	1.197	1.747	0.497	0.895	0.492	1.234
ERK1/2 (Thr202/Tyr204)	1.303	1.234	1.236	1.748	0.193	1.496	1.469	0.996
FOXO1/ FOXO3 (Thr24/Thr32)	0.000	0.000	0.730	12.885	0.000	1.788	0.000	0.498
Histone H2AX (Ser139)	0.000	0.000	0.000	0.000	0.000	0.099	1.655	0.000
IGF1Rb (Tyr1131), INSRb (Tyr1146)	1.685	0.906	1.084	1.370	0.455	1.034	0.881	1.055
IGF1Rb (Tyr1135), INSRb (Tyr1136)	2.679	0.724	1.677	2.083	0.843	1.649	0.458	1.025
Ku80	1.575	1.567	1.084	2.293	0.470	0.984	0.982	1.048
LC3B	1.953	1.327	1.261	1.481	0.419	0.887	1.630	1.084
MEK1/2 (Ser217/Ser22)	1.300	1.486	1.869	1.534	0.264	0.986	1.253	1.037
mTOR (Ser2448)	1.603	1.151	1.678	1.573	0.451	1.285	0.884	1.061
Neutrophil Elastase	1.303	2.019	0.943	1.850	0.466	1.623	1.543	1.135
NRF2	1.880	1.321	1.300	2.565	0.624	1.267	0.524	1.776
p70 S6K (Thr389)	0.922	1.645	1.666	2.732	1.125	1.893	0.193	0.768
PDL1	1.468	0.856	1.066	1.454	0.556	0.816	0.698	0.923
PI3K p110y	1.317	1.474	0.930	1.517	0.140	1.212	1.657	1.165
pS6RP (Ser235/Ser236)	0.941	0.746	2.595	2.052	0.217	1.015	0.321	0.880
Rad51	1.372	2.296	2.311	2.590	1.476	0.922	0.655	0.941
Rad54	1.238	2.298	1.298	2.347	1.071	1.179	0.760	1.078
RASGRF1 (Ser916)	2.722	1.024	2.161	3.037	0.540	1.317	0.511	1.535
SAPK/JNK (Thr183/Tyr185)	0.000	0.000	0.000	0.000	0.000	0.000	2.837	0.000

APPENDIX 3

Supplemental Table 3: Wilcoxon paired testing analyzing the protein expression of baseline/pre-PIKTOR vs disease progressed/post-PIKTOR microdissected tumor biopsy samples in 8 patients. Patients 6 and 8 were excluded because both lack a matched pre-PIKTOR tumor samples.

Endpoints	Pre-PIKTOR Expression (n)	Pre-PIKTOR Expression (mean)	Pre-PIKTOR Expression (stdev)	Post-PIKTOR Expression (n)	Post-PIKTOR Expression (Mean)	Post-PIKTOR Expression (stdev)	P value	Adjusted P Value
53BP1	8	0.349	1.064	8	-0.203	0.996	0.250	1.00
AKT (Ser473)	8	0.017	0.707	8	0.110	1.353	0.945	1.00
Androgen Receptor (AR)	8	0.072	1.109	8	-0.420	0.606	0.109	0.97
BRCA1	8	0.181	1.283	8	-0.351	0.523	0.461	1.00
BRCA2	8	0.070	1.080	8	0.067	1.034	1.000	1.00
CD45	8	0.143	1.292	8	-0.066	0.814	0.641	1.00
CDK2	8	0.055	1.193	8	-0.033	0.958	0.383	1.00
Cleaved PARP (Asp214)	8	0.114	1.227	8	0.034	0.899	1.000	1.00
DNA-PKcs	8	0.126	1.150	8	-0.051	0.819	0.844	1.00
EGFR (Thr654)	8	0.131	1.006	8	-0.325	1.002	0.461	1.00
EGFR (Tyr1173)	8	0.215	1.431	8	-0.219	0.469	0.383	1.00
ErbB2/HER2 (Tyr1248)	8	0.602	0.952	8	-0.459	0.824	**0.039**	0.72
ErbB3/HER3 (Tyr1289) (21D3)	8	-0.112	0.991	8	-0.148	0.972	0.844	1.00
ERK1/2 (Thr202/Tyr204)	8	0.224	1.209	8	-0.176	0.782	0.250	1.00
FOXO1/ FOXO3 (Thr24/Thr32)	8	-0.027	0.917	8	0.204	1.181	0.742	1.00
Histone H2AX (Ser139)	8	0.279	1.086	8	-0.144	1.025	0.438	1.00

IGF1Rb (Tyr1131), INSRb (Tyr1146)	8	-0.033	1.231	8	-0.138	0.822	0.844	1.00
IGF1Rb (Tyr1135), INSRb (Tyr1136)	8	-0.062	0.342	8	-0.177	1.418	0.547	1.00
Ku80	8	0.298	1.011	8	-0.120	0.730	0.313	1.00
LC3B	8	0.304	1.343	8	-0.426	0.478	0.250	1.00
MEK1/2 (Ser217/Ser22)	8	0.202	1.205	8	-0.120	0.840	0.250	1.00
mTOR (Ser2448)	8	0.233	1.174	8	-0.120	0.873	0.383	1.00
Neutrophil Elastase	8	0.323	1.192	8	-0.549	0.511	0.109	0.97
NRF2	8	0.256	1.327	8	-0.340	0.551	0.383	1.00
p70 S6K (Thr389)	8	-0.002	0.840	8	0.071	1.263	0.742	1.00
PDL1	8	-0.034	1.246	8	0.012	0.932	0.742	1.00
PI3K p110y	8	0.078	1.309	8	-0.244	0.714	0.250	1.00
pS6RP (Ser235/Ser236)	8	-0.037	1.101	8	-0.001	0.928	0.641	1.00
Rad51	8	0.156	1.129	8	-0.328	0.892	0.250	1.00
Rad54	8	0.516	1.235	8	-0.374	0.504	**0.078**	0.92
RASGRF1 (Ser916)	8	0.353	1.346	8	-0.324	0.519	0.148	0.99
SAPK/JNK (Thr183/Tyr185)	8	0.272	1.285	8	-0.123	0.757	0.625	1.00

APPENDIX 4

Supplement Table 4: Wilcoxon paired testing analyzing the protein expression of baseline/pre-PIKTOR vs disease progressed/post-PIKTOR microdissected tumor biopsy samples in 7 patients. Patients 6 and 8 were excluded because both lack a matched pre-PIKTOR tumor samples; patient 9 was excluded as an outlier in the data.

Endpoints	Pre-PIKTOR Expression (n)	Pre-PIKTOR Expression (mean)	Pre-PIKTOR Expression (stdev)	Post-PIKTOR Expression (n)	Post-PIKTOR Expression (Mean)	Post-PIKTOR Expression (stdev)	P value	Adjusted P Value
53BP1	7	-0.144	1.060	7	0.168	1.007	0.375	0.999
AKT (Ser473)	7	-0.137	1.253	7	-0.114	0.650	0.578	0.999
Androgen Receptor (AR)	7	-0.610	0.305	7	-0.239	0.731	0.219	0.991
BRCA1	7	-0.397	0.547	7	0.402	1.209	0.156	0.972
BRCA2	7	0.125	1.103	7	0.195	1.102	0.813	1.000
CD45	7	-0.164	0.826	7	0.199	1.385	0.297	0.997
CDK2	7	-0.114	1.005	7	0.432	0.577	**0.078**	0.879
Cleaved PARP (Asp214)	7	0.122	0.932	7	0.182	1.309	0.813	1.000
DNA-PKcs	7	-0.210	0.738	7	0.301	1.121	0.375	0.999
EGFR (Thr654)	7	-0.357	1.077	7	0.267	1.004	0.375	0.999
EGFR (Tyr1173)	7	-0.278	0.473	7	0.372	1.469	0.156	0.972
ErbB2/HER2 (Tyr1248)	7	-0.485	0.886	7	0.808	0.812	**0.016**	0.396
ErbB3/HER3 (Tyr1289) (21D3)	7	-0.243	1.008	7	0.070	0.915	0.469	0.999
ERK1/2 (Thr202/Tyr204)	7	-0.218	0.835	7	0.566	0.784	**0.031**	0.626
FOXO1/ FOXO3 (Thr24/Thr32)	7	0.343	1.202	7	0.066	0.949	0.688	0.999
Histone H2AX (Ser139)	7	-0.074	1.087	7	0.408	1.104	0.438	0.999

IGF1Rb (Tyr1131), INSRb (Tyr1146)	7	-0.176	0.880	7	0.343	0.670	0.375	0.999
IGF1Rb (Tyr1135), INSRb (Tyr1136)	7	-0.275	1.502	7	-0.076	0.367	0.469	0.999
Ku80	7	-0.193	0.755	7	0.511	0.877	**0.078**	0.879
LC3B	7	-0.497	0.469	7	0.653	0.982	**0.047**	0.726
MEK1/2 (Ser217/Ser22)	7	-0.154	0.901	7	0.442	1.075	**0.031**	0.626
mTOR (Ser2448)	7	-0.225	0.887	7	0.427	1.122	**0.078**	0.879
Neutrophil Elastase	7	-0.508	0.537	7	0.668	0.739	**0.031**	0.626
NRF2	7	-0.360	0.591	7	0.423	1.339	0.219	0.991
p70 S6K (Thr389)	7	0.046	1.362	7	-0.069	0.884	0.938	1.000
PDL1	7	-0.165	0.848	7	-0.021	1.345	1.000	1.000
PI3K p110y	7	-0.321	0.733	7	0.466	0.771	**0.031**	0.626
pS6RP (Ser235/Ser236)	7	-0.147	0.899	7	0.062	1.151	1.000	1.000
Rad51	7	-0.287	0.955	7	0.191	1.214	0.375	0.999
Rad54	7	-0.364	0.543	7	0.629	1.289	0.109	0.922
RASGRF1 (Ser916)	7	-0.387	0.526	7	0.504	1.377	**0.078**	0.879
SAPK/JNK (Thr183/Tyr185)	7	-0.054	0.790	7	0.397	1.335	0.625	0.999

APPENDIX 5

Supplemental table 5: Mann Whitney U (MWU) test analyzing the protein expression of pre- and post-PIKTOR tumor samples. Patients were stratified on whether they experienced stable disease (SD) or disease progression (PD) after cis+nab-pac. SD (patients 1, 4, 8, 10) were stable for ≥ 20 weeks after treatment with PIKTOR and Chemotherapy; PD (patients 2, 5, 6, 9, 11, 12) were stable for < 20 weeks.

Endpoints	SD Patient Pre-PIKTOR (n)	SD Patient Pre-PIKTOR Expression (mean)	SD Patient Pre-PIKTOR Expression (stdev)	PD Patient Pre-PIKTOR (n)	PD Patient Pre-PIKTOR Expression (mean)	PD Patient Pre-PIKTOR Expression (stdev)	P value	Adjusted P Value
53BP1	3	-0.664	0.433	5	0.073	1.178	0.250	0.999
AKT (Ser473)	3	-0.692	0.315	5	0.591	1.543	0.393	0.999
Androgen Receptor (AR)	3	-0.792	0.417	5	-0.197	0.624	0.250	0.999
BRCA1	3	-0.770	0.608	5	-0.099	0.289	0.143	0.987
BRCA2	3	-0.353	0.827	5	0.319	1.148	0.393	0.999
CD45	3	-0.587	0.258	5	0.247	0.895	0.250	0.999
CDK2	3	-0.043	0.694	5	-0.027	1.169	1.000	1.000
Cleaved PARP (Asp214)	3	0.934	0.931	5	-0.507	0.082	**0.036**	0.688
DNA-PKcs	3	-0.613	0.613	5	0.287	0.779	0.250	0.999
EGFR (Thr654)	3	-0.495	0.927	5	-0.222	1.136	0.786	1.000
EGFR (Tyr1173)	3	-0.529	0.336	5	-0.033	0.462	0.250	0.999
ErbB2/HER2 (Tyr1248)	3	-0.628	0.881	5	-0.358	0.875	0.571	1.000
ErbB3/HER3 (Tyr1289) (21D3)	3	-0.683	0.962	5	0.173	0.921	0.786	1.000
ERK1/2 (Thr202/Tyr204)	3	-0.440	0.367	5	-0.018	0.959	0.571	1.000
FOXO1/ FOXO3 (Thr24/Thr32)	3	1.400	1.120	5	-0.514	0.312	**0.036**	0.688

Histone H2AX (Ser139)	3	0.326	1.654	5	-0.426	0.455	0.732	1.000
IGF1Rb (Tyr1131), INSRb (Tyr1146)	3	-0.227	1.285	5	-0.084	0.589	0.786	1.000
IGF1Rb (Tyr1135), INSRb (Tyr1136)	3	-1.075	0.519	5	0.362	1.555	0.143	0.987
Ku80	3	-0.619	0.641	5	0.179	0.654	0.143	0.987
LC3B	3	-0.512	0.634	5	-0.374	0.436	0.786	1.000
MEK1/2 (Ser217/Ser22)	3	-0.692	0.364	5	0.224	0.881	0.250	0.999
mTOR (Ser2448)	3	-0.926	0.490	5	0.365	0.658	**0.071**	0.883
Neutrophil Elastase	3	-0.403	0.656	5	-0.637	0.464	0.571	1.000
NRF2	3	-0.666	0.335	5	-0.144	0.589	0.143	0.987
p70 S6K (Thr389)	3	-0.779	0.351	5	0.582	1.364	0.143	0.987
PDL1	3	-0.486	0.628	5	0.311	1.012	0.250	0.999
PI3K p110y	3	-0.009	0.384	5	-0.385	0.867	0.786	1.000
pS6RP (Ser235/Ser236)	3	-0.636	0.287	5	0.380	0.991	0.250	0.999
Rad51	3	-0.882	0.122	5	0.004	1.008	0.250	0.999
Rad54	3	-0.660	0.406	5	-0.202	0.513	0.250	0.999
RASGRF1 (Ser916)	3	-0.845	0.238	5	-0.011	0.343	**0.036**	0.688
SAPK/JNK (Thr183/Tyr185)	3	0.031	1.092	5	-0.214	0.614	1.000	1.000

REFERENCES

1. C. E. DeSantis, J. Ma, M. M. Gaudet, L. A. Newman, K. D. Miller, A. G. Sauer, A. Jemal, R. L. Siegel, Breast cancer statistics, 2019. *CA: A Cancer Journal for Clinicians*. **69**, 438–451 (2019).

2. J. Makki, Diversity of Breast Carcinoma: Histological Subtypes and Clinical Relevance. *Clin Med Insights Pathol*. **8**, 23–31 (2015).

3. M. A. Medina, G. Oza, A. Sharma, L. G. Arriaga, J. M. Hernández Hernández, V. M. Rotello, J. T. Ramirez, Triple-Negative Breast Cancer: A Review of Conventional and Advanced Therapeutic Strategies. *Int J Environ Res Public Health*. **17** (2020), doi:10.3390/ijerph17062078.

4. G. Bianchini, J. M. Balko, I. A. Mayer, M. E. Sanders, L. Gianni, Triple-negative breast cancer: challenges and opportunities of a heterogeneous disease. *Nature Reviews Clinical Oncology*. **13**, 674–690 (2016).

5. K. Pogoda, A. Niwińska, M. Murawska, T. Pieńkowski, Analysis of pattern, time and risk factors influencing recurrence in triple-negative breast cancer patients. *Med Oncol*. **30** (2013), doi:10.1007/s12032-012-0388-4.

6. N. Howlader, A. Noone, D. Miller, A. Brest, M. Yu, J. Ruhl, Z. Tatalovich, A. Mariotto, D. Lewis, H. Chen, E. Feuer, K. Cronin, SEER Cancer Statistics Review. *National Cancer Institute* (2017) (available at https://seer.cancer.gov/csr/1975_2017/).

7. R. Dent, M. Trudeau, K. I. Pritchard, W. M. Hanna, H. K. Kahn, C. A. Sawka, L. A. Lickley, E. Rawlinson, P. Sun, S. A. Narod, Triple-Negative Breast Cancer: Clinical Features and Patterns of Recurrence. *Clin Cancer Res*. **13**, 4429–4434 (2007).

8. B. D. Lehmann, J. A. Bauer, X. Chen, M. E. Sanders, A. B. Chakravarthy, Y. Shyr, J. A. Pietenpol, Identification of human triple-negative breast cancer subtypes and preclinical models for selection of targeted therapies. *J Clin Invest*. **121**, 2750–2767 (2011).

9. M. Bonotto, L. Gerratana, E. Poletto, P. Driol, M. Giangreco, S. Russo, A. M. Minisini, C. Andreetta, M. Mansutti, F. E. Pisa, G. Fasola, F. Puglisi, Measures of Outcome in Metastatic Breast Cancer: Insights From a Real-World Scenario. *Oncologist*. **19**, 608–615 (2014).

10. W. D. Foulkes, I. E. Smith, J. S. Reis-Filho, Triple-Negative Breast Cancer. *New England Journal of Medicine*. **363**, 1938–1948 (2010).

11. S. P. Shah, A. Roth, R. Goya, A. Oloumi, G. Ha, Y. Zhao, G. Turashvili, J. Ding, K. Tse, G. Haffari, A. Bashashati, L. M. Prentice, J. Khattra, A. Burleigh, D. Yap, V. Bernard, A. McPherson, K. Shumansky, A. Crisan, R. Giuliany, A. Heravi-Moussavi, J. Rosner, D. Lai, I. Birol, R. Varhol, A. Tam, N. Dhalla, T. Zeng, K. Ma, S. K. Chan, M. Griffith, A. Moradian, S.-W. G. Cheng, G. B. Morin, P. Watson, K. Gelmon, S. Chia, S.-F. Chin, C. Curtis, O. M. Rueda, P. D. Pharoah, S. Damaraju, J. Mackey, K. Hoon, T. Harkins, V. Tadigotla, M. Sigaroudinia, P. Gascard, T. Tlsty, J. F. Costello, I. M. Meyer, C. J. Eaves, W. W. Wasserman, S. Jones, D. Huntsman, M. Hirst, C. Caldas, M. A. Marra, S. Aparicio, The clonal and mutational evolution spectrum of primary triple-negative breast cancers. *Nature*. **486**, 395–399 (2012).

12. D. W. Craig, J. A. O'Shaughnessy, J. A. Kiefer, J. Aldrich, S. Sinari, T. M. Moses, S. Wong, J. Dinh, A. Christoforides, J. L. Blum, C. L. Aitelli, C. R. Osborne, T. Izatt, A. Kurdoglu, A. Baker, J. Koeman, C. Barbacioru, O. Sakarya, F. M. De La Vega, A. Siddiqui, L. Hoang, P. R. Billings, B. Salhia, A. W. Tolcher, J. M. Trent, S. Mousses, D. Von Hoff, J. D. Carpten, Genome and transcriptome sequencing in prospective metastatic triple-negative breast cancer uncovers therapeutic vulnerabilities. *Mol Cancer Ther*. **12**, 104–116 (2013).

13. K. Yoshida, Y. Miki, Role of BRCA1 and BRCA2 as regulators of DNA repair, transcription, and cell cycle in response to DNA damage. *Cancer Science*. **95**, 866–871 (2004).

14. A. Prat, C. Cruz, K. A. Hoadley, O. Díez, C. M. Perou, J. Balmaña, Molecular features of the basal-like breast cancer subtype based on BRCA1 mutation status. *Breast Cancer Res Treat*. **147**, 185–191 (2014).

15. H. Davies, D. Glodzik, S. Morganella, L. R. Yates, J. Staaf, X. Zou, M. Ramakrishna, S. Martin, S. Boyault, A. M. Sieuwerts, P. T. Simpson, T. A. King, K. Raine, J. E. Eyfjord, G. Kong, Å. Borg, E. Birney, H. G. Stunnenberg, M. J. van de Vijver, A.-L. Børresen-Dale, J. W. M. Martens, P. N. Span, S. R. Lakhani, A. Vincent-Salomon, C. Sotiriou, A. Tutt, A. M. Thompson, S. Van Laere, A. L. Richardson, A. Viari, P. J. Campbell, M. R. Stratton, S. Nik-Zainal, HRDetect is a predictor of BRCA1 and BRCA2 deficiency based on mutational signatures. *Nature Medicine*. **23**, 517–525 (2017).

16. J. S. Brown, B. O'Carrigan, S. P. Jackson, T. A. Yap, Targeting DNA Repair in Cancer: Beyond PARP Inhibitors. *Cancer Discov*. **7**, 20–37 (2017).

17. H. H. Y. Chang, N. R. Pannunzio, N. Adachi, M. R. Lieber, Non-homologous DNA end joining and alternative pathways to double-strand break repair. *Nature Reviews Molecular Cell Biology*. **18**, 495–506 (2017).

18. H. Wang, L. Z. Shi, C. C. L. Wong, X. Han, P. Y.-H. Hwang, L. N. Truong, Q. Zhu, Z. Shao, D. J. Chen, M. W. Berns, J. R. Y. Iii, L. Chen, X. Wu, The Interaction of

CtIP and Nbs1 Connects CDK and ATM to Regulate HR–Mediated Double-Strand Break Repair. *PLOS Genetics*. **9**, e1003277 (2013).

19. J.-H. Seol, E. Y. Shim, S. E. Lee, Microhomology-mediated end joining: Good, bad and ugly. *Mutat Res*. **809**, 81–87 (2018).

20. J. Saha, A. J. Davis, Unsolved mystery: the role of BRCA1 in DNA end-joining. *J Radiat Res*. **57**, i18–i24 (2016).

21. F. Chen, Y. Li, N. Qin, F. Wang, J. Du, C. Wang, F. Du, T. Jiang, Y. Jiang, J. Dai, Z. Hu, C. Lu, H. Shen, RNA-seq analysis identified hormone-related genes associated with prognosis of triple negative breast cancer. *J Biomed Res*. **34**, 129–138 (2020).

22. J. M. Mulligan, L. A. Hill, S. Deharo, G. Irwin, D. Boyle, K. E. Keating, O. Y. Raji, F. A. McDyer, E. O'Brien, M. Bylesjo, J. E. Quinn, N. M. Lindor, P. B. Mullan, C. R. James, S. M. Walker, P. Kerr, J. James, T. S. Davison, V. Proutski, M. Salto-Tellez, P. G. Johnston, F. J. Couch, D. Paul Harkin, R. D. Kennedy, Identification and Validation of an Anthracycline/Cyclophosphamide–Based Chemotherapy Response Assay in Breast Cancer. *J Natl Cancer Inst*. **106** (2014), doi:10.1093/jnci/djt335.

23. N. Johnson, Y.-C. Li, Z. E. Walton, K. A. Cheng, D. Li, S. J. Rodig, L. A. Moreau, C. Unitt, R. T. Bronson, H. D. Thomas, D. R. Newell, A. D. D'Andrea, N. J. Curtin, K.-K. Wong, G. I. Shapiro, Compromised CDK1 activity sensitizes BRCA-proficient cancers to PARP inhibition. *Nature Medicine*. **17**, 875–882 (2011).

24. M. Castroviejo-Bermejo, C. Cruz, A. Llop-Guevara, S. Gutiérrez-Enríquez, M. Ducy, Y. H. Ibrahim, A. Gris-Oliver, B. Pellegrino, A. Bruna, M. Guzmán, O. Rodríguez, J. Grueso, S. Bonache, A. Moles-Fernández, G. Villacampa, C. Viaplana, P. Gómez, M. Vidal, V. Peg, X. Serres-Créixams, G. Dellaire, J. Simard, P. Nuciforo, I. T. Rubio, R. Dienstmann, J. C. Barrett, C. Caldas, J. Baselga, C. Saura, J. Cortés, O. Déas, J. Jonkers, J.-Y. Masson, S. Cairo, J.-G. Judde, M. J. O'Connor, O. Díez, J. Balmaña, V. Serra, A RAD51 assay feasible in routine tumor samples calls PARP inhibitor response beyond BRCA mutation. *EMBO Mol Med*. **10** (2018), doi:10.15252/emmm.201809172.

25. Y. H. Ibrahim, C. García-García, V. Serra, L. He, K. Torres-Lockhart, A. Prat, P. Anton, P. Cozar, M. Guzmán, J. Grueso, O. Rodríguez, M. T. Calvo, C. Aura, O. Díez, I. T. Rubio, J. Pérez, J. Rodón, J. Cortés, L. W. Ellisen, M. Scaltriti, J. Baselga, PI3K Inhibition Impairs BRCA1/2 Expression and Sensitizes BRCA-Proficient Triple-Negative Breast Cancer to PARP Inhibition. *Cancer Discov*. **2**, 1036–1047 (2012).

26. J. Pascual, N. C. Turner, Targeting the PI3-kinase pathway in triple-negative breast cancer. *Annals of Oncology*. **30**, 1051–1060 (2019).

27. L. M. Thorpe, H. Yuzugullu, J. J. Zhao, PI3K in cancer: divergent roles of isoforms, modes of activation, and therapeutic targeting. *Nat Rev Cancer*. **15**, 7–24 (2015).

28. C. Cintas, J. Guillermet-Guibert, Heterogeneity of Phosphatidylinositol-3-Kinase (PI3K)/AKT/Mammalian Target of Rapamycin Activation in Cancer: Is PI3K Isoform Specificity Important? *Front. Oncol.* **7** (2018), doi:10.3389/fonc.2017.00330.

29. C. Denkert, C. Liedtke, A. Tutt, G. von Minckwitz, Molecular alterations in triple-negative breast cancer-the road to new treatment strategies. *Lancet*. **389**, 2430–2442 (2017).

30. D. Juric, J. S. de Bono, P. M. LoRusso, J. Nemunaitis, E. I. Heath, E. L. Kwak, T. M. Mercadé, E. Geuna, M. J. de Miguel-Luken, C. Patel, K. Kuida, S. Sankoh, E. H. Westin, F. Zohren, Y. Shou, J. Tabernero, A First-in-Human, Phase I, Dose-Escalation Study of TAK-117, a Selective PI3Kα Isoform Inhibitor, in Patients with Advanced Solid Malignancies. *Clin Cancer Res*. **23**, 5015–5023 (2017).

31. H. A. Burris, C. D. Kurkjian, L. Hart, S. Pant, P. B. Murphy, S. F. Jones, R. Neuwirth, C. G. Patel, F. Zohren, J. R. Infante, TAK-228 (formerly MLN0128), an investigational dual TORC1/2 inhibitor plus paclitaxel, with/without trastuzumab, in patients with advanced solid malignancies. *Cancer Chemother Pharmacol*. **80**, 261–273 (2017).

32. F. Musa, A. Alard, G. David-West, J. P. Curtin, S. V. Blank, R. J. Schneider, Dual mTORC1/2 inhibition as a novel strategy for the re-sensitization and treatment of platinum-resistant ovarian cancer. *Mol Cancer Ther*. **15**, 1557–1567 (2016).

33. V. Espina, J. D. Wulfkuhle, V. S. Calvert, A. VanMeter, W. Zhou, G. Coukos, D. H. Geho, E. F. Petricoin, L. A. Liotta, Laser-capture microdissection. *Nature Protocols*. **1**, 586–603 (2006).

34. V. Espina, K. H. Edmiston, M. Heiby, M. Pierobon, M. Sciro, B. Merritt, S. Banks, J. Deng, A. J. VanMeter, D. H. Geho, L. Pastore, J. Sennesh, E. F. Petricoin, L. A. Liotta, A Portrait of Tissue Phosphoprotein Stability in the Clinical Tissue Procurement Process. *Mol Cell Proteomics*. **7**, 1998–2018 (2008).

35. C. P. Paweletz, L. Charboneau, V. E. Bichsel, N. L. Simone, T. Chen, J. W. Gillespie, M. R. Emmert-Buck, M. J. Roth, E. F. Petricoin Iii, L. A. Liotta, Reverse phase protein microarrays which capture disease progression show activation of pro-survival pathways at the cancer invasion front. *Oncogene*. **20**, 1981–1989 (2001).

36. A. J. VanMeter, A. S. Rodriguez, E. D. Bowman, J. Jen, C. C. Harris, J. Deng, V. S. Calvert, A. Silvestri, C. Fredolini, V. Chandhoke, E. F. Petricoin, L. A. Liotta, V. Espina, Laser Capture Microdissection and Protein Microarray Analysis of Human Non-small Cell Lung Cancer. *Mol Cell Proteomics*. **7**, 1902–1924 (2008).

37. K. M. Sheehan, V. S. Calvert, E. W. Kay, Y. Lu, D. Fishman, V. Espina, J. Aquino, R. Speer, R. Araujo, G. B. Mills, L. A. Liotta, E. F. Petricoin, J. D. Wulfkuhle, Use of Reverse Phase Protein Microarrays and Reference Standard Development for Molecular Network Analysis of Metastatic Ovarian Carcinoma *. *Molecular & Cellular Proteomics*. **4**, 346–355 (2005).

38. A. Bahrami, M. Khazaei, S. Shahidsales, S. M. Hassanian, M. Hasanzadeh, M. Maftouh, G. A. Ferns, A. Avan, The Therapeutic Potential of PI3K/Akt/mTOR Inhibitors in Breast Cancer: Rational and Progress. *Journal of Cellular Biochemistry*. **119**, 213–222 (2018).

39. V. Serra, M. Scaltriti, L. Prudkin, P. J. A. Eichhorn, Y. H. Ibrahim, S. Chandarlapaty, B. Markman, O. Rodriguez, M. Guzman, S. Rodriguez, M. Gili, M. Russillo, J. L. Parra, S. Singh, J. Arribas, N. Rosen, J. Baselga, PI3K inhibition results in enhanced HER signaling and acquired ERK dependency in HER2-overexpressing breast cancer. *Oncogene*. **30**, 2547–2557 (2011).

40. K. E. O'Reilly, F. Rojo, Q.-B. She, D. Solit, G. B. Mills, D. Smith, H. Lane, F. Hofmann, D. J. Hicklin, D. L. Ludwig, J. Baselga, N. Rosen, mTOR Inhibition Induces Upstream Receptor Tyrosine Kinase Signaling and Activates Akt. *Cancer Res*. **66**, 1500–1508 (2006).

41. B. D. Lehmann, J. A. Bauer, J. M. Schafer, C. S. Pendleton, L. Tang, K. C. Johnson, X. Chen, J. M. Balko, H. Gómez, C. L. Arteaga, G. B. Mills, M. E. Sanders, J. A. Pietenpol, PIK3CA mutations in androgen receptor-positive triple negative breast cancer confer sensitivity to the combination of PI3K and androgen receptor inhibitors. *Breast Cancer Research*. **16**, 406 (2014).

42. L. Yin, J.-J. Duan, X.-W. Bian, S. Yu, Triple-negative breast cancer molecular subtyping and treatment progress. *Breast Cancer Research*. **22**, 61 (2020).

43. A. Hernández-Prat, A. Rodriguez-Vida, N. Juanpere-Rodero, O. Arpi, S. Menéndez, L. Soria-Jiménez, A. Martínez, N. Iarchouk, F. Rojo, J. Albanell, R. Brake, A. Rovira, J. Bellmunt, Novel Oral mTORC1/2 Inhibitor TAK-228 Has Synergistic Antitumor Effects When Combined with Paclitaxel or PI3Kα Inhibitor TAK-117 in Preclinical Bladder Cancer Models. *Mol Cancer Res*. **17**, 1931–1944 (2019).

44. H. Li, X. Li, S. Liu, L. Guo, B. Zhang, J. Zhang, Q. Ye, Programmed cell death-1 (PD-1) checkpoint blockade in combination with a mammalian target of rapamycin inhibitor restrains hepatocellular carcinoma growth induced by hepatoma cell–intrinsic PD-1. *Hepatology*. **66**, 1920–1933 (2017).

45. S. Adams, P. Schmid, H. S. Rugo, E. P. Winer, D. Loirat, A. Awada, D. W. Cescon, H. Iwata, M. Campone, R. Nanda, R. Hui, G. Curigliano, D. Toppmeyer, J. O'Shaughnessy, S. Loi, S. Paluch-Shimon, A. R. Tan, D. Card, J. Zhao, V. Karantza,

J. Cortés, Pembrolizumab monotherapy for previously treated metastatic triple-negative breast cancer: cohort A of the phase II KEYNOTE-086 study. *Annals of Oncology*. **30**, 397–404 (2019).

46. S. Loi, S. Adams, P. Schmid, J. Cortés, D. W. Cescon, E. P. Winer, D. L. Toppmeyer, H. S. Rugo, M. D. Laurentiis, R. Nanda, H. Iwata, A. Awada, A. Tan, A. Wang, G. Aktan, V. Karantza, R. Salgado, Relationship between tumor infiltrating lymphocyte (TIL) levels and response to pembrolizumab (pembro) in metastatic triple-negative breast cancer (mTNBC): Results from KEYNOTE-086. *Annals of Oncology*. **28**, v608 (2017).

47. C. Mueller, A. Haymond, J. B. Davis, A. Williams, V. Espina, Protein biomarkers for subtyping breast cancer and implications for future research. *Expert Rev Proteomics*. **15**, 131–152 (2018).

48. R. R. Langley, I. J. Fidler, The seed and soil hypothesis revisited—The role of tumor-stroma interactions in metastasis to different organs. *International Journal of Cancer*. **128**, 2527–2535 (2011).

49. S. Das, A. W. Lo, Re-inventing drug development: A case study of the I-SPY 2 breast cancer clinical trials program. *Contemporary Clinical Trials*. **62**, 168–174 (2017).

50. J. J. Chan, T. J. Y. Tan, R. A. Dent, Novel therapeutic avenues in triple-negative breast cancer: PI3K/AKT inhibition, androgen receptor blockade, and beyond. *Ther Adv Med Oncol*. **11** (2019), doi:10.1177/1758835919880429.

51. P. Giovannelli, M. Di Donato, G. Galasso, E. Di Zazzo, A. Bilancio, A. Migliaccio, The Androgen Receptor in Breast Cancer. *Front Endocrinol (Lausanne)*. **9** (2018), doi:10.3389/fendo.2018.00492.

52. M. Rampurwala, K. B. Wisinski, R. O'Regan, Role of the Androgen Receptor in Triple-Negative Breast Cancer. *Clin Adv Hematol Oncol*. **14**, 186–193 (2016).

53. F. Sobande, L. Dušek, A. Matějková, T. Rozkoš, J. Laco, A. Ryška, EGFR in triple negative breast carcinoma: significance of protein expression and high gene copy number. *Cesk Patol*. **51**, 80–86 (2015).

54. T. M. Severson, D. M. Wolf, C. Yau, J. Peeters, D. Wehkam, P. C. Schouten, S.-F. Chin, I. J. Majewski, M. Michaut, A. Bosma, B. Pereira, T. Bismeijer, L. Wessels, C. Caldas, R. Bernards, I. M. Simon, A. M. Glas, S. Linn, L. van 't Veer, The BRCA1ness signature is associated significantly with response to PARP inhibitor treatment versus control in the I-SPY 2 randomized neoadjuvant setting. *Breast Cancer Res*. **19** (2017), doi:10.1186/s13058-017-0861-2.

55. R. Bartsch, E. de Azambuja, I-SPY 2: optimising cancer drug development in the 21st century. *ESMO Open*. **1**, e000113 (2016).

BIOGRAPHY

Tuong Vi V. Nguyen received her Bachelor of Science in Biology from George Mason University in 2020. She went on to receive her Master in the same field, with a concentration in translational clinical research at George Mason in 2021. She has 2 years of experience in undergraduate and graduate research.